energies

Review

Parameters Affecting Dust Collector Efficiency for Pneumatic Conveying: A Review

Philippe Beaulac [1,*], Mohamad Issa [2], Adrian Ilinca [3] and Jean Brousseau [1]

1 Department of Engineering, Université du Québec à Rimouski, Rimouski, QC G5L 3A1, Canada; jean_brousseau@uqar.ca
2 Department of Applied Sciences, Quebec Maritime Institute, Rimouski, QC G5L 4B4, Canada; missa@imq.qc.ca
3 Laboratoire de Recherche en Énergie Éolienne (LREE), Université du Québec à Rimouski, Rimouski, QC G5L 3A1, Canada; adrian_ilinca@uqar.ca
* Correspondence: pbeaup@gmail.com

Abstract: In a context of energy abundance for industrial applications, industrial systems are exploited with minimal attention to their actual energy consumption requirements to meet the loads imposed on them. As a result, most of them are used at maximal capacity, regardless of the varying operational conditions. First, the paper studies pneumatic conveying systems and thoroughly reviews previously published work. Then, we overview simulations and operating data of the experimental parameters and their effects on the flow characteristics and transport efficiency. Finally, we summarize with a conclusion and some suggestions for further work. The primary goal of this study is to identify the parameters that influence the energy consumption of industrial dust collector systems. It is differentiated from previously published overviews by being concentrated on wood particles collection systems. The results will permit a better selection of an appropriate methodology or solution for reducing an industrial system's power requirements and energy consumption through more precise control. The anticipated benefits are not only on power requirement and energy consumption but also in reducing greenhouse gas emissions. This aspect shows more impacts in regions that rely on electricity supplied by thermal power stations, especially those that use petrol or coal.

Keywords: fluid mechanics; pneumatic conveying; multiphase flows; dust collector; industrial control; energy efficiency

Citation: Beaulac, P.; Issa, M.; Ilinca, A.; Brousseau, J. Parameters Affecting Dust Collector Efficiency for Pneumatic Conveying: A Review. *Energies* **2022**, *15*, 916. https://doi.org/10.3390/en15030916

Academic Editor: Dmitry Eskin

Received: 31 December 2021
Accepted: 23 January 2022
Published: 27 January 2022

1. Introduction

Constantly evolving technology offers many new possibilities for industrial process optimization. Industrial production systems are prone to design and upgrade research in an attempt to increase their productivity or decrease their input needs in terms of resources, whether it be human intervention or energy consumption.

According to the Energy Information Administration of the US Department of Energy [1,2], and summarized in Table 1, the industrial sector consumes 32.53% of the overall energy consumption worldwide.

Table 1. Energy consumption by sector, 2019 [1].

Sector	Petawatt-Hours	Percentage
Residential	20.98	20.98
Commercial	17.94	17.94
Industrial	95.75	32.53
Transportation	84.02	28.55
Total	272.43	100

It does not only represent the electricity consumption, but with such a high proportion, it becomes highly justifiable to put effort into increasing the energy efficiency of industrial applications. These efforts should be prioritized in areas where the energy production emits high concentrations of greenhouse gas (GHG).

Furthermore, extensive research on energy consumption [3] has outlined figures on energy consumption and global electricity production by source. From these figures, we can notice that fossil fuel consumption represents 84.33% of all energy consumption in the world as of 2019 (Figure 1) and that 67.03% of global electricity production comes from fossil fuels (Figure 2).

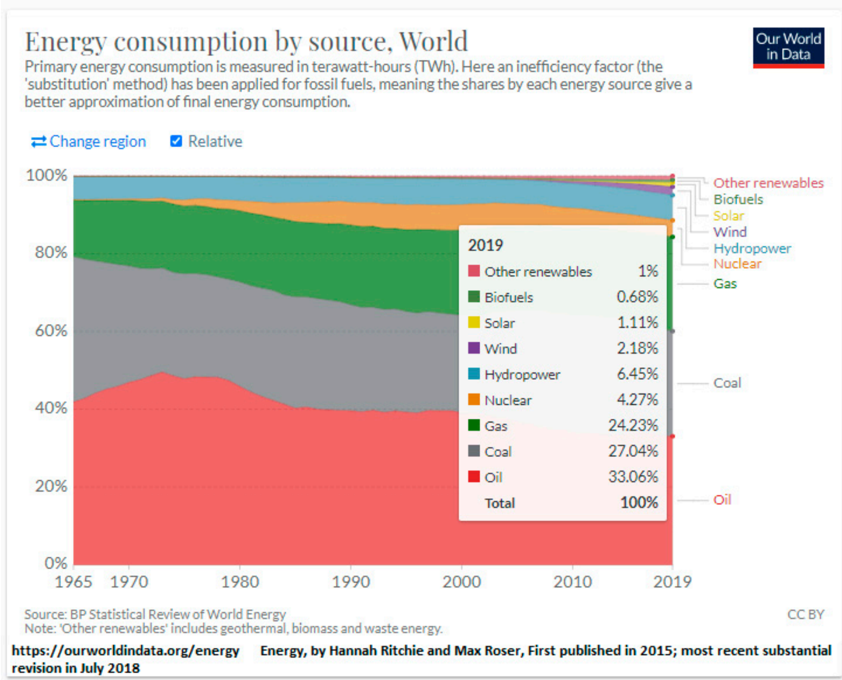

Figure 1. Energy consumption in the world, 2019.

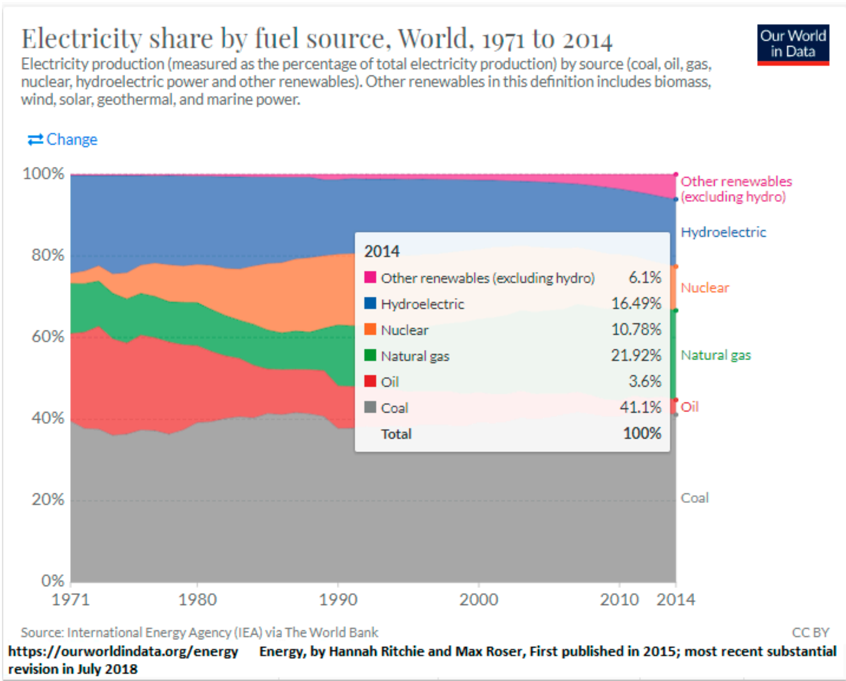

Figure 2. Global electricity production distribution.

These high percentages and the increasingly pressing need to diminish our GHG emissions more than justify efforts to optimize industrial energy consumptions through better accuracy of their control strategies. Other incentives become more and more pressing as climate changes are widely felt. These take the form of regulations such as taxes, subsidies, tradable emission permits, and green certificates, as outlined by Bunse [4].

To improve the energy efficiency of an industrial system, one possible avenue is by better controlling its energy consumption by optimizing it according to the production needs. The operating costs of industrial systems are directly associated with the electrical energy consumed.

Many industrial applications consume more energy than required to respond to demands. One can refer to dust collection systems and compressed air systems that almost always show leaks [5]. These systems tend to run at 100% capacity for the duration of the production periods.

This surplus of consumption can seem low, if regarded per industrial system, but becomes considerably high when considering the whole factory, with all its systems. If a control strategy allows for the reduction of the gap between input and output, the benefits can only be increased.

Industrial systems consume energy to manipulate the load imposed on them and to operate actions that serve to improve the value of the input resources. The energy levels necessary to fulfill these actions often vary with time; hence, they must be monitored and adjusted, if an interest is placed in the efficiency of the system.

The first part of an efficiency analysis must then be emphasized on the system itself and its operation parameters, using strategically selected performance indicators. This selection should be made on a basis of the chosen parameters to optimize, and a benchmarking strategy should be prioritized. Bunse et al. have explored the energy efficiency indicators and benchmarking strategies in their paper [4] by drafting an overview of research and needs on the general subject of energy efficiency. Accordingly, it becomes obvious that there are needs for developing more intelligent control strategies to optimize energy efficiency of industrial systems.

Furthermore, an overview of the system's architecture and physical configuration must be assessed to be able to determine what parameters will help to efficiently monitor the system's operation to respond to the load imposed on it. A textbook approach can be applied, as the one proposed in Modeling and Analysis of Dynamic Systems [6], from which the parameters and machine variables should emerge. The physics of the implicated activities of the system should be well identified because this will lead to the optimization methods to be applied. If modeling developments are required, they will be based on the analysis of the physical phenomena identified. The culmination of the optimization process of any industrial system for the ultimate objective of improving its energy efficiency must tend towards better and more precise controlling strategies.

Whether it is soft controls or hard controls, as defined by Naidu and Rieger [7,8], or a combination of the two, the optimal solution must be adapted for the industrial system of the study. The exact type of control to implement should be selected after a thorough analysis of the system. This analysis must be conducted according to the particularities of the system and the various technologies as well as the physics implied in its design. A modeling strategy can prove to be a valuable tool for the analysis and design of the control strategy by reproducing the response of the system to adjustments made for energy efficiency.

One of the main concerns for developing an adapted control system is the relevance and precision of the data that is considered for the optimal adjustments. In the case of dust collectors, the obvious goal is to adjust the energy output of the source, to consume just the necessary amount of energy, at all moments of operation. The challenge lies in the evaluation of the real charge imposed on the dust collector's electric motor as a basis for the adjustments to be made to the power consumption of the system.

This paper will attempt to draw an overview of the influencing parameters which have an impact on the energy consumption of dust collector systems. A subsequent study will be elaborated to explore the control avenues that can lead to optimal energy efficiency.

In Section 2, we present a portrait of the state of the art of studies regarding dust collector systems. This section will emphasize the structure of a typical dust collecting system, starting with a global view of all components, and follow with a more detailed description of the cyclones and their influence on the performance of the system. This section also outlines the particularities of pneumatic conveying systems and the parameters that best influence the overall system's efficiency. Section 3 presents a general conclusion and further research possibilities.

2. State of the Art

2.1. Dust Collector System Overview

Dust collecting systems are composed of three main sub-systems:

1. The cyclone with its centrifugal pump (fan) and filter units (bags)
2. The dust evacuation sub-system (airlock and dust disposal)
3. The dust collection and transport circuits (cut-off valves (blast gates) and ducting)

Figure 3 shows the main components of a dust collecting system.

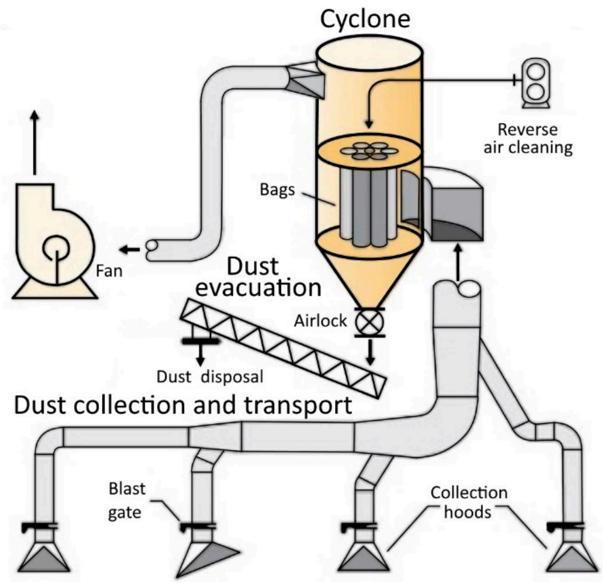

Figure 3. Schematic of a dust collection system.

A dust collection system removes the dust contents of an industrial environment to provide a comfortable work environment and meet safety and health regulations. The system takes the dust particles and carries them outside for disposal or reuse possibilities.

The system has a power unit that develops the necessary work for the collection and transport of the particles and the separation of the dust particles from their carrying fluid, usually air. This power unit is the electric motor and fan attached to the cyclone, which separates the two phases of the flow, i.e., (i) the dust and the transporting fluid, and; (ii) the air. This power unit utilizes a ducting network to transport the dust from the collection points throughout the plant. When designing the ducting network, careful considerations must be taken to achieve a high-efficiency pneumatic conveying of the dust particles. Modern systems tend to use controlling strategies to save energy by closing specific areas of the ducting circuit that do not require dust removal. One of these systems consists of gate valves, operated by pneumatic energy, which close the ducts at strategically selected points in the circuit. This efficiency strategy is coupled with a variable frequency drive control that can reduce the motor's speed to meet the required dust collection needs.

The dust evacuation sub-system comprises a rotating airlock valve that transfers the dust particles from the dust collector to the dust disposal mechanism and isolates the evacuation duct from the cyclone chamber. The dust disposal mechanism serves to evacuate the dust particles to a container, which can be taken away from the factory to disposal sites or alternate users. Since this sub-system has limited influence on the overall performance of the dust collection system, its details will be omitted in this study. Emphasis will be put on the cyclone unit and the ducting circuit. The performance of the dust collecting system relies on the proper transport of the dust in the collecting ducts and the adequate separation of the dust from the transporting medium, in our case, air. The energy-consuming component of a dust collection system is the electric motor that implements the rotation conditions for the centrifugal pump, the fan, the most critical element of the system, producing the airflow necessary to transport the dust particles to the dust collector. The efficiency and energy consumption of the electric motor are directly linked to the behavior of the upstream components, the ducting, and the collection hoods. Unfortunately, typical dust collector systems do not present the means to adjust the electric motor's velocity. Dust collector manufacturers offer the option of adding a variable frequency drive, which can significantly improve the system's overall efficiency.

The influential parameters for proper dust collection are the velocities of the air flow in the ducts, directly dependent on the differential pressures present in the various locations in the system. Other parameters that could influence the performance of the system are the density of dust present in the ducts, the shape and size of the dust particles, the temperature and the humidity of the flow [9,10]. According to Clarke's study [9], there is a 0.16 m/s difference in the fluidization velocity of sawdust particles containing moisture ranging from 8% to 82%, which appears to present minimal effect. Kunii's Fluidization Engineering manual [10] points out the influence of the void fraction between particles on the fluidization velocities. This critical parameter of the flow increases by up to 8% for temperatures up to 500 °C for fine particles, but is unaffected for coarse particles, which is the case for sawdust particles. These two last parameters have a significantly smaller influence on the performance of the system than the rest of the enumerated parameters, so they will be set aside for the scope of this study.

Dust collectors and pneumatic conveying have been developed and used in industrial transport applications for well over 100 years. The technology emerged from the invention of the Roots blower (Figure 4), which was first tried in 1859 by the Roots brothers in the U.S. [11], and it is still widely used in modern pneumatic conveying applications, although it has been continually tested and upgraded into what we know of it today.

Figure 4. Roots blower [12].

Let's look at the two main technologies used by this industrial application: the cyclone of the dust collector itself, which serves to separate the dust from the airflow, and the pneumatic conveying circuit, which serves to transport the particles to the dust collector.

2.2. Cyclones

The cyclone is an integral part of the power source of the dust collecting system. It serves a general purpose of separating the two phases of the flow: the solid phase is deposited in the bottom to be later evacuated from the system, and the gas phase is recirculated back into the system, or simply exhausted to the environment during periods of higher ambient temperatures. Obviously, the recirculation of the exhaust air to the plant in colder periods allows for the retention of a portion of the thermal charge of the air for heating efficiency purposes.

A cyclone is generally of cylindrical shape, with a cone at its bottom to collect the solid phase. The dimensions of the cyclone are established according to the performance desired and the type of application it will be subjected to, as explained by Leith [13]. The dimensioning criteria are the height and width of the inlet conduit, the ratio of the heights of the cylindrical and conical parts, and ratios in relation to the overall diameter of the cyclone.

The multiphase flow enters the cyclone and forms a vortex that forces the solid particles to adhere to the inner walls of the cylindrical part of the cyclone. When the particles are subjected to boundary layer conditions, they fall to the bottom of the conical part to be evacuated out of the cyclone.

The overall efficiency of the cyclone is mainly given by its ability to separate the two phases of the flow, as defined by Azadi [14]: it is referred to as the separation rate. It is expressed via the rate of settling of particles according to their size. Obviously, the smaller the size of the particle that can be separated by the cyclone, the better the efficiency of this cyclone, as can be deduced by observing the cyclone grade efficiency of Figure 5 [13].

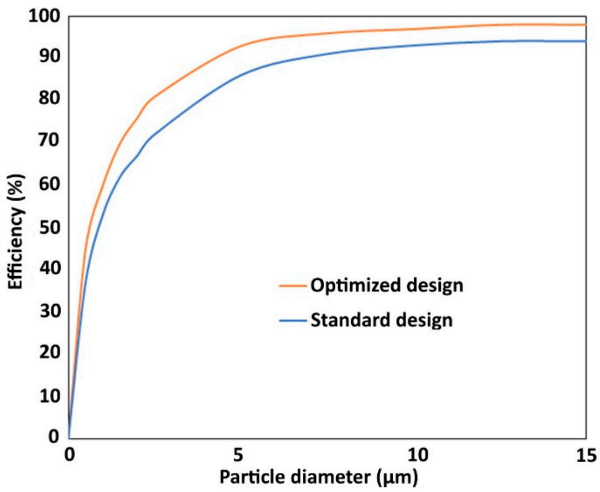

Figure 5. Cyclone efficiency curves, standard and optimized design [13].

The separation is produced by a cyclonic movement of the multiphase flow. The dynamics of the cyclonic movement permits the separation of the particles of the solid phase from the flow, which falls to the bottom of the dust collector. The specific details of this physical phenomenon have been studied and experimented by C.B. Shepherd and C.E. Lapple and documented in 1939 [15], and reviewed by A.J. ter Linden in 1949 [16]. Shepherd and Lapple studied the pressure drop in the cyclone in relation to its design, which is defined as the difference between the pressure at the cyclone inlet and the average pressure across the outlet [14]. Linden concentrated more on the relation between the various velocity profiles and the rates of settling of particles in the cyclone. Linden's experiments demonstrated that a lower rate of settling indicates a greater separating capacity.

The rate of settling of a particle according to its size can be computed from Stoke's law of deposition [16]

$$V_g = \frac{\delta^2 g}{18} \frac{(s_1 - s_2)}{\mu} \cong \frac{\delta^2 g s_1}{18\mu} \tag{1}$$

where

V_g = rate of settling (m/s)
s_1 = density of particles in the flow (kg/m^3)
s_2 = density of gas (air in our case, hence negligeable) (kg/m^3)
δ = diameter of particle assumed spherical (m)

g = acceleration due to gravity (m/s^2)
μ = viscosity of gas [kg/(m·s)]

This representation of the rate of settling refers to the size of the smallest particle, which can be separated. Therefore, a high efficiency cyclone has a low rate of settling. The rate of settling can also be expressed as a relation between the radial and tangential velocities (V_r and V_t, respectively) of a particle on a trajectory of the radius r [16].

$$V_g = \frac{grV_r}{V_t^2} \tag{2}$$

Variations of the Equations (1) and (2) have been explored to simplify its use, in the fields of sedimentology [17] and aerosol deposition in working environments [18].

The flow of fluid transporting solid particles enters the cyclone at a velocity that can be determined by the speed of the dust collector's fan. As the flow is diverted by the inner surface of the cylindrical part of the cyclone, the tangential velocity of the flow is diminished and the particles either cling to the inner surface or drop to the bottom of the cyclone in a spiral trajectory because of boundary layer conditions [16].

From the layout of Figure 6 and Equation (2), we can see that the tangential velocity has an important influence on the particle trajectory and thereby its separation rate. As the tangential velocity increases, the rate of settling decreases and hence the cyclone efficiency increases.

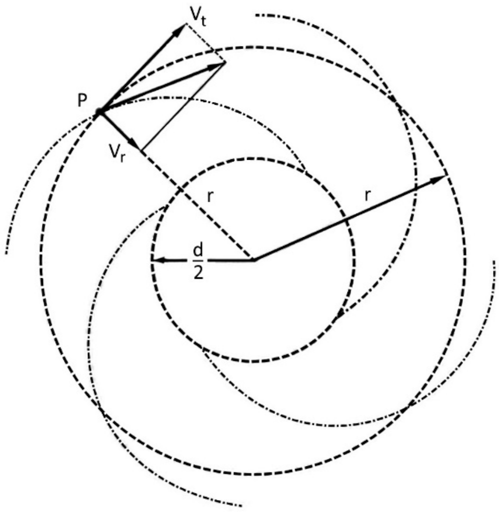

Figure 6. Flow around the exhaust of a cyclone [16].

A particle P enters a cyclone of radius r with tangential and radial velocities V_t and V_r. Its tangential velocity decreases and the particle is separated from the transporting medium, air, which exhausts the cyclone from outlet of radius d/2.

It becomes clear that a varying tangential velocity will influence the settling of particles, hence the overall efficiency of the cyclone. This has been simulated in Azadi's CFD study on cyclone performance parameters [19], and Figure 7 shows parts of the results that this study produced. It is clearly demonstrated that the velocity increases towards the cyclone wall.

The optimization of the cyclone performance relies on the dust particle sizes and shapes, and also the densities of the solid phase, as pointed out in Leith's cyclone performance study [13]. Figure 5 shows efficiency curves of cyclone designs according to particle sizes.

In the cyclone efficiency curves presented, the efficiency relates to the weight of particles of a stated size collected, divided by the total weight of those particles entering the cyclone. Thus, it gives the separation efficiency of the cyclone for given sizes of particles. We can clearly conclude that the efficiency increases with increasing particle size.

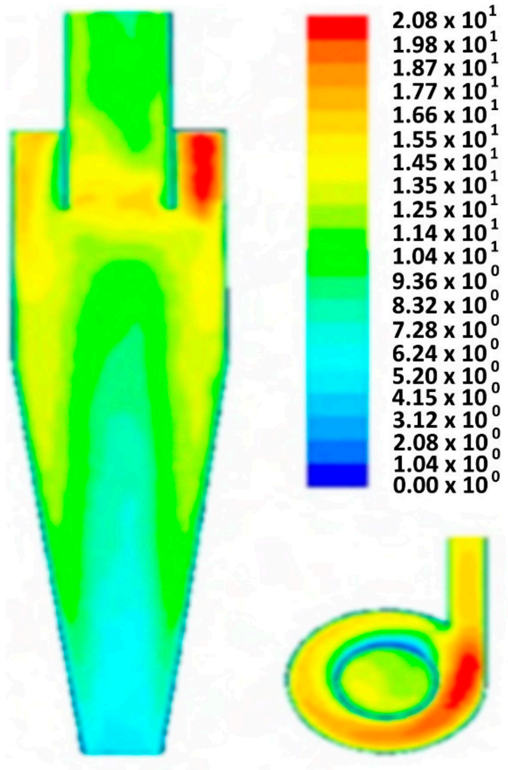

Figure 7. Velocity magnitudes [19].

The most influential parameter for optimal separation remains the velocity of the flow at the entrance of the cyclone, which is controlled by adjusting the speed of the fan's electric motor. It is, therefore, pertinent to verify its impact on the overall efficiency of the cyclone since it will be the major adjustment parameter of this analysis. According to the graph in Figure 8, the pressure drop increases as the inlet gas velocity increases. These curves were obtained for both an empirical and a numerical solution. The material used was typical cement raw material. The characteristic diameter of particle used was 29.9 μm and the particle density was 3320 kg/m^3.

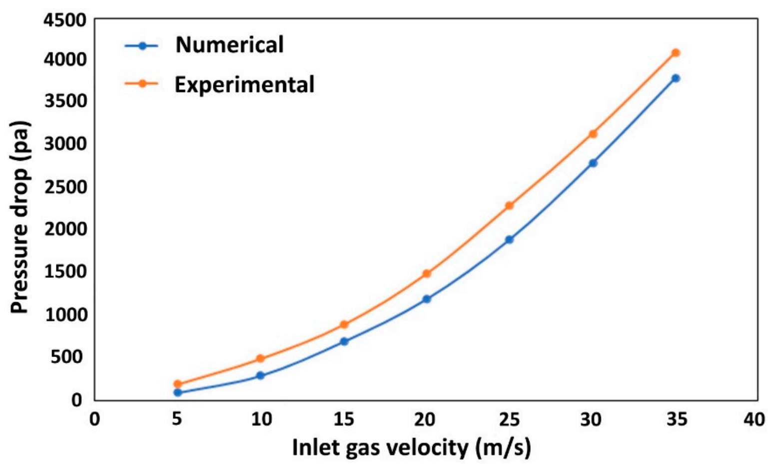

Figure 8. The influence of the inlet velocities on the pressure drop in the cyclone [20].

It has also been studied and simulated by Huang and al. [21] that the increase of dust density affects the hydrodynamics and separation capacities of a cyclone. From their experiments and simulations, they confirmed that if the density of the particle phase of the flow increases, it will have a reducing effect on the pressure drop and the tangential velocity in the cyclone, and an increasing effect on its separation efficiency. This is explained by the presence of larger particles, which cause a sweeping effect on the smaller particles and result in higher localization of these particles near the wall region of the cyclone, where the separation efficiency is higher. This relationship will have to be taken into account in the control strategy to be developed.

The effects of the variations of the pressure drops on the overall performance of the cyclone are thus felt mostly on its separating capacities. According to Wang et al. [20], the separation efficiency of the cyclone is related to the inlet velocity of the flow, which in turn also affects the pressure drop. This effect was also confirmed by Huang et al. [21] and other authors (Shepherd and Lapple [15], Coker [22]) as summarized in the chart of Figure 9.

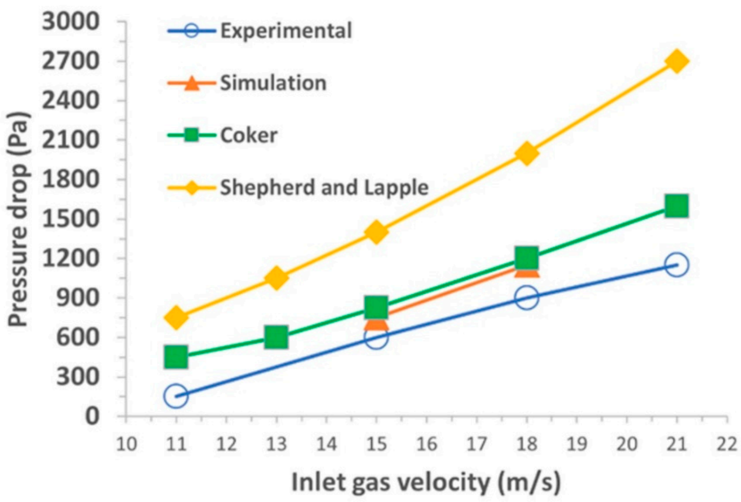

Figure 9. Comparisons of pressure drops.

The negative effect of this last observation reaches the main concern of this study, which is the energy efficiency of the dust collector system. As Funk et al. [23] pointed out, the energy consumption of the dust collector is directly proportional to the pressure drop in the cyclone. With these reviews, it is possible to draw a picture of the interaction between the parameters. This will be very useful to consider when developing the models and the control strategy for the system.

It can be concluded from this short review of cyclone collectors that the independent parameters of the system are the cyclone geometry, the inlet gas velocity, the particle density as well as their size distribution; the dependent parameters that are affected by these are the pressure loss, the separating efficiency and the general energy costs of the system.

These parameters have effects on each other, which of course affect the overall efficiency of the cyclone. Gimbun et al. [24] pointed out that a higher inlet velocity yields a higher cyclone efficiency but also increases the pressure drop across the cyclone. So, an acceptable setting for the inlet velocity will also affect the pressure drop. The inlet velocity is controlled by the rotation speed of the electric motor that propels the fan of the system. This adjustment must not fall below a certain value at which point the efficiency of the cyclone starts to be critically low. This threshold can be determined by the particles parameters, i.e., density, shape and size. This relationship between the inlet velocity, the pressure drop and the cyclone efficiency has been studied through computational fluid dynamics (CFD) using empirical models [25] and, more recently, commercial-coding software such as Fluent [14,24]. There seems to be a lack of research for developing a control algorithm that can help to determine this threshold, in real-time, so manufacturers and service technicians tend to set a generalized value of 50%.

If the inlet velocity is reduced to meet the requirements of the system's charge, the pressure drop in the cyclone will also diminish, hence reducing the power consumption of the dust collector. Additionally, with a reducing inlet velocity and/or increased density of the particle phase, the separation capacity of the cyclone will also be affected. The critical point to respect then becomes a target not to exceed. The relationship between the different cyclone parameters of interest is depicted in the following statement.

$$\rho \nearrow \Rightarrow \Delta p \searrow, v_t \searrow, V_g \nearrow$$

2.3. Pneumatic Conveying

The principle of pneumatic conveying rests on the transport properties of a fluid, usually air, to efficiently carry bulk products from a point of delivery to a point of transformation. Setting aside the cyclone and filtering system which serve to separate the solid phase from the fluid phase, the pneumatic conveying system is composed of a turbine, blower or fan, and a network of ducts. The turbine produces the fluid movement, and the ducting directs the solids to the discharge point. This transport method is often preferred to mechanical conveyors because of its lower equipment costs and ease of maintenance [26].

The principle rests on the action of fluidization of beds of particles: a fluid flows through a packed bed of particles at sufficient velocities to loosen the particles and carry them in a particle-fluid mixture that behaves very much like a single-phased fluid [10,27]. The fluidization can be divided into distinct regimes. The first fluidization phase can be described as air being forced through a bed of particles causing a pressure drop across the bed. As the pressure drop increases, it becomes sufficient to support the particles in suspension in the air flow: this is the minimum fluidization velocity. If the air flow continues to increase, formation of bubbles occurs, in which the particles are carried. These bubbles will become slugs (or plugs) when the velocity continues to increase [28].

Many studies have been conducted in the field of pneumatic conveying [10,11,26,29–31]. Older studies present the technology and its necessary equipment, and advancement in this regard has been limited to the performances of the turbine and the design calculations of the duct sizes and network configuration. Early studies in pneumatic conveying emerged from Germany and Japan. Klinzing [26] outlined that accurate predictive models need to be developed for pneumatic conveying systems.

The design parameters that direct a particular pneumatic conveying system are imposed by the particles to be carried. According to Klinzing [26], it is important to consider the properties of the particles to be carried in the system, prior to its design:

- Average particle size and size distribution;
- Percent of particles <200 μm;
- Assessment of the characteristic of stickiness;
- Moisture content;
- True density and bulk density of the particles.

The main element of the problem rests on the nature of the flow in the system. The charge on the system is directly proportional to the quantity of material to transport, but also pertains to the configuration of the ducting network and the surrounding conditions (temperature, humidity, atmospheric pressure).

Multiphase flows composed of a solid and a gas phase are primarily characterized by their solid particle contents. According to the volume fraction α_s (Equation (3)) of the solid phase of the flow, it can be characterized as a dilute or dense flow,

$$\alpha_s = \frac{V_s}{V_{cell}} \tag{3}$$

where

V_s = volume of the particles in a specific cell
V_{cell} = volume of the cell.

The volume of particles in a specific cell can be calculated from the density measurement of the multiphase flow. The ratio of the volumes, or the volume fraction as defined in Equation (3), is equal to the ratio of the measured density and the particles density, as described in Equation (4),

$$\frac{V_s}{V_{cell}} = \frac{\rho_m}{\rho_p} \tag{4}$$

where

ρ_m = measured density of the multiphase flow
ρ_p = density of the wood particles

Using a cell volume of 1 m^3 and using the particles density measured according to a method described by Abdullah and Geldart [32], we can directly determine the volume ratio of the flow. One possible way of measuring the flow density would be to use a mechanical vibration non-intrusive densitometer [33]. Other measuring strategies may not be suitable for solids-gas multiphase flows.

Schellander [34] established a relationship between the calculation method with respect to the density of the flow of particles. This calculation method then directs the model design for the flow to study. A dilute flow that has a particle volume fraction lower than 10^{-6} can be considered regardless of their effects on the gas flow and on their mutual collision effects. If the volume fraction is between 10^{-6} and 0.5, the influence of the particles will greatly affect the gas flow and must be considered in the analysis and modeling. The exchanges between the gas flow and the particle flow must be included and the particle phase is considered as a source of mass, momentum and energy in regards to the fluid phase. If the volume fraction is greater than 0.5, the flow is considered to be dense, and the particle-particle interactions must be included in the simulation model and calculation.

According to this classification, the Lagrangian particle tracing method is used for dilute flows and the Eulerian particulate phase model is used for the dense flows [34]. The equations for these modeling methods will be explored in Section 2.4. Figure 10 depicts this classification.

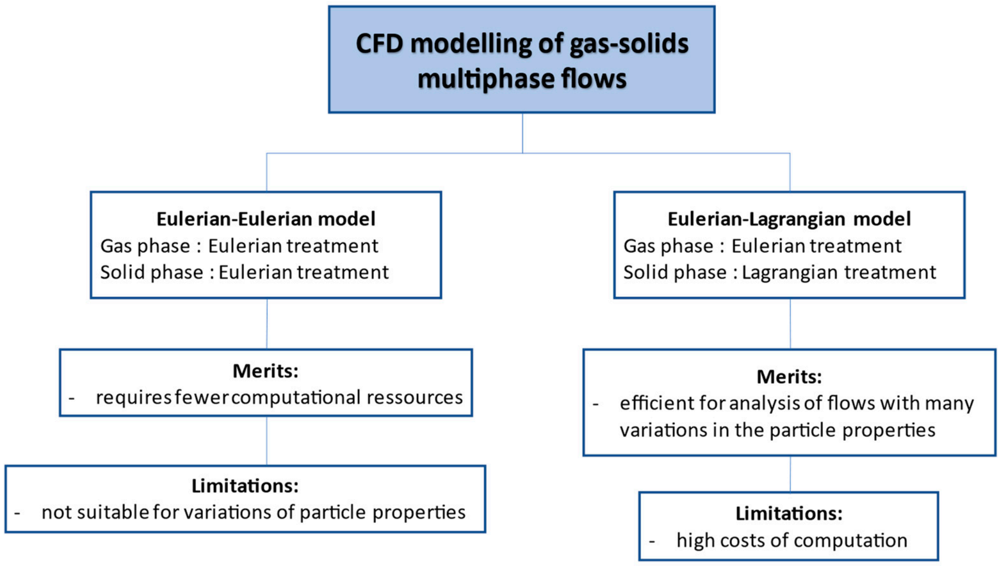

Figure 10. Particle-laden flow regimes, adapted from [35].

Further studies of dilute versus dense multiphase flows have been developed by Manjula et al. [35] with an emphasis on the modeling techniques, and it also takes into account the nature of the solid phase. The two main modeling techniques are outlined and compared, according to the particle-particle interactions and the particle properties. These two methods are the Eulerian–Eulerian approach and the Eulerian–Lagrangian approach. Figure 11 summarizes the differences between the two methods.

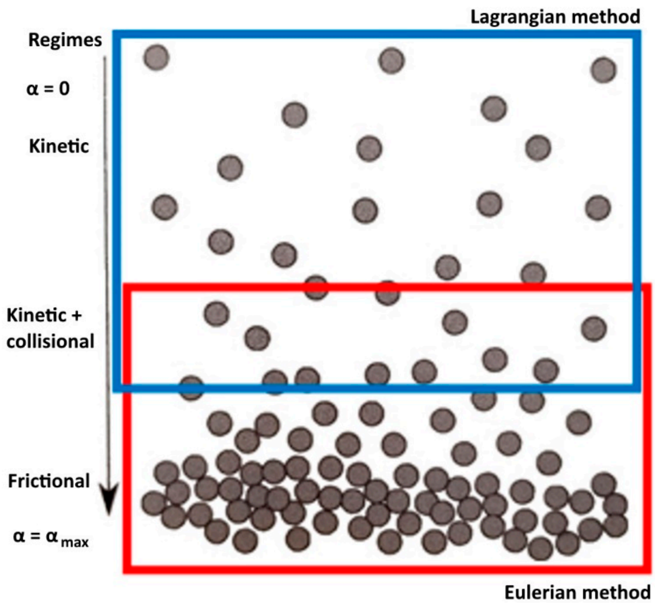

Figure 11. CFD modeling comparison [35].

The maximum values of the volume fraction of a flow of mono-dispersed spherical particles is $\alpha_s = 0.64$ [34,36]. This can give a limit density to respect, but in a wood particle collecting system, considering the relatively random shapes of the particles, and their range of sizes, this limit value should be revised. This subject presents certain possibilities for future research projects.

The increase of particle density in the flow will affect the mode of transport by changing the flow pattern. Figure 12 shows sketches of the possible patterns of flow in ducts, adapted from Wen [37], established from observation of glass bead flows.

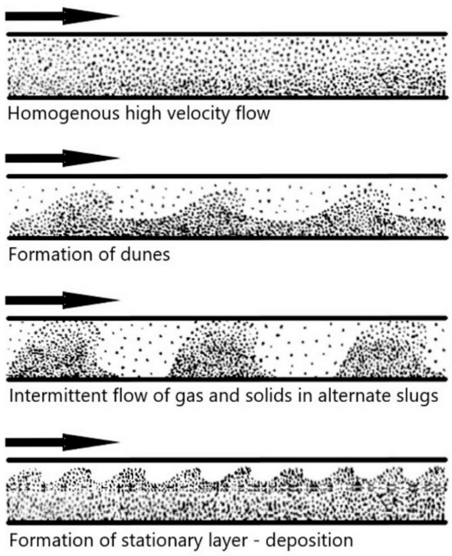

Figure 12. Flow patterns for glass beads [37].

The profiles shown in these flow patterns demonstrate the impact of the transport velocities on the overall performance of the system. When the velocity is sufficient to transport all the particles in the flow, the distribution of particles in the duct is homogenous and there is little deposition.

Manjula et al. [35] describe the difference in dilute and dense flows: in dilute multiphase flows, the bulk of the particles are transported by being suspended in the transporting gas; if the gas velocity is reduced, the flow of particles starts to display dune-like features or definite plugs of particles, and most of the particles are no longer suspended in the transporting gas. This last situation describes a dense multiphase flow. From this description, one can readily assume that the effect of varying density will also affect the flow of particles.

As the density of particles increases, or inversely as the velocity decreases, the flow starts to segregate into regions of higher density, and the formation of dunes takes place. Further increase of the density will develop a slug flow and eventually the formation of a stationary layer of particles in the duct [37].

The relationship between the pressure and the velocity can be associated with the density of particles in the flow. The behavior of pressure in a flow is similar to that of a potential difference in an electric circuit: the more there are resistances in the circuit, the bigger the potential difference, and similarly, the more there are resistances to the free flow of the fluid in the pipes, the higher the pressure differential [38].

A dilute particle phase will present very little resistance to the flow, hence low pressure buildup. Additionally, since the flow does not contain many particles, the velocity is maximum, being affected very little. Inversely, if the particle phase is dense, it means there are more particles to carry, hence more resistance to the flow, and higher pressure. In this case, the velocity is greatly affected by the dense particle phase. This is based on the principles of conservation of energy and explained by Thomson [31].

As illustrated in Figure 13, dense particle phase flows can present an accumulation of particles into plugs that can still be transported, provided that the system can produce enough power to meet the charge of particles.

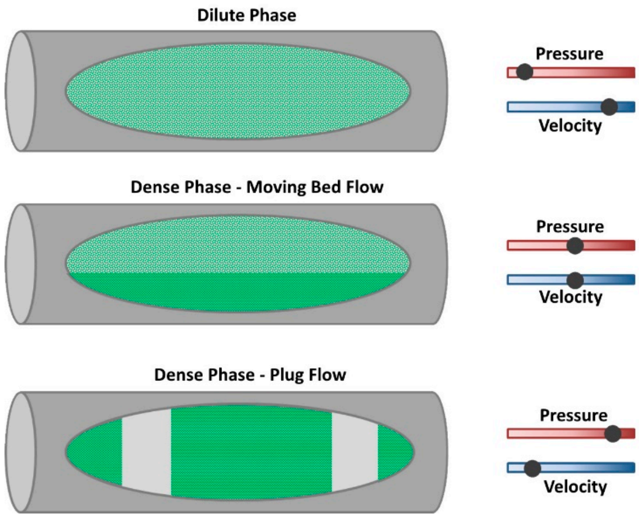

Figure 13. Dilute vs dense phase flow—https://www.ddpsinc.com/knowledge/are-there-different-types-of-pneumatic-conveying-systems (accessed on 7 May 2019).

To improve the efficiency of a dust collecting system, it becomes imperative to determine the type of flow that is optimal, in order to set the parameters for the standards we want to reach. In a study of the prediction modes of flow in pneumatic conveying systems, Jones and Williams [30] established that the optimal mode of flow is a dense particle phase flow, rather than a dilute phase flow. Dense particle flows can be distinguished between two classes: a fluidized dense phase, which is characterized by a high air retention and low permeability, and a plug-type (or slug-type) flow for materials that de-aerate quickly and possess a high permeability [30].

Williams pointed out that in general, pneumatic conveying can have negative effects on the material being conveyed, such as degradation or attrition, and negative effects on the system, such as erosive wear. These effects will have more risks of occurring at high velocities and dilute phase conveying [39]. Another downfall of high-velocity dilute phase flow is the amount of energy required to generate the velocity. Lower velocities are directly linked to the rotating speed of the electric motor and lead to more economical operation of the system.

Jones and Williams [30] address a review of the flow type prediction methods developed. These methods rely on a grouping strategy of the particle types according to similar properties of their behavior when fluidized by a gas (A, B, C and D types of particles) first proposed by Geldart [40], and complemented by Dixon [41], Molerus [42] and Pan [43], generally based on the density differences and mean size of particles. They differentiate bulk density from particle density: bulk density is calculated by dividing the total mass of a specific material by the volume it occupies [44]. This takes into account the presence of a fluid or other particles between the measured particles themselves. In the case of a gas-solid multiphase flow, the particles are intertwined with air pockets.

The group A type particles have a small mean size and a low particle bulk density, usually less than 1.4 g/cm^3. The behavior of this group shows particle bed expansion before the formation of transport bubbles starts. The bubbles rise more rapidly than the interstitial gas velocity. The collapse of this type of particle flow is generally slow [40]. The rising velocity of the bubbles can be determined by Equation (5) [45], which puts in relationship the minimum bubble forming velocity u_b, the bubble size d_b and a shape factor k_1 that varies between 0.8 and 1.2:

$$u_b = k_1 \left(\frac{1}{2} g d_b \right)^{\frac{1}{2}} \tag{5}$$

The group B type particles are situated in a range of mean size between 40 and 500 μm, and in a range of bulk densities between 1.4 and 4 g/cm^3. The bubbles from this group of particles form at, or slightly above, the minimum fluidization velocity, which is the main difference with the group A particles. This particularity influences the formation of slug transport, which is more closely related to the gas velocity for fluidization than the bubble rise velocity. A "slug" (or plug) flow is characterized by a moving packed bed of particles in the pipe and usually takes up all the space; hence, it has the same diameter as the pipe itself [38].

The group C type particles show inter-particle cohesion, which renders this type of flow much more difficult to fluidize. Finally, the group D type particles are characterized by their large mean size and/or high density.

This classification was used by many researchers (Dixon, 1979 [41]; Geldart, 1973 [40]; Molerus, 1982 [42]; Williams and Jones, 2003 [46]; Pan, 1999 [43]) [30] to produce flow prediction charts. Further research (Jones, 1988; Mainwaring and Reed, 1987) [30] introduced the behavior of the particles in a multiphase flow, in terms of permeability and air retention. The particles are then classified according to their ability to present a fluidized dense phase flow. With this new criterion, they explore the existing classification techniques used to predict the mode of flow of particle-laden flows. Table 2 presents a summary of the predictive capability of these techniques [30], considering only loose-poured bulk density (and permeability) instead of the actual particle density and the mean particle size. The table characterizes the traced graphs from all different researchers. It is divided into strong predictive regions and transition regions. Therefore, according to the type of solid phase encountered, the graph and table can approximate the type of flow to expect.

Two of the classification techniques presented can serve to predict the flow of all four types of powders in all types of flow. They are the modified Geldart and modified Molerus fluidization diagrams. The two present the same flow regions, with a slight difference in the boundaries between the types of powders. Molerus presents a chart with adjusted boundaries after taking into account the forces due to the particles' collisions. Hence, it is more accurate than Geldart's diagram, and it is the one presented in this paper (see Figure 14).

Table 2. Summary of mode of flow predictive capability of basic bulk material diagrams [30].

Diagram	Strong Predictive Regions			Transition Regions
	Fluidized Dense Phase	**Dilute Only**	**Plug Flow**	
Geldart	A and C powder groups	No prediction	D-type powders with $(\rho_s - \rho_a) < 2000\ \mathrm{kg/m^3}$	B-type powders, D-type powders with $(\rho_s - \rho_a) < 2000\ \mathrm{kg/m^3}$
Modified Geldart	A and C powder groups	B powders with $\rho_{blp} > 1000\ \mathrm{kg/m^3}$	D-type powders	B-type powders with $\rho_{blp} > 1000\ \mathrm{kg/m^3}$
Molerus	A and C powder groups	No prediction	D-type powders with $(\rho_s - \rho_a) < 2000\ \mathrm{kg/m^3}$	B-type powders, D-type powders with $(\rho_s - \rho_a) < 2000\ \mathrm{kg/m^3}$
Modified Molerus	A and C powder groups	B powders with $\rho_{blp} > 1000\ \mathrm{kg/m^3}$	D-type powders	B-type powders with $\rho_{blp} > 1000\ \mathrm{kg/m^3}$
Dixon (Ø50 − 100 mm pipes)	No slugging behavior	No prediction	Axisymmetric slugging and D > 100 mm i.d. $(\rho_s - \rho_a) < 2000\ \mathrm{kg/m^3}$	Slightly less accurate than the Geldart and Molerus models
Modified Dixon (Ø50 − 100 mm pipes)	No slugging behavior	Asymmetric slugging and $\rho_{blp} > 1000\ \mathrm{kg/m^3}$	Axisymmetric slugging and D > 100mm i.d.	Slightly less accurate than the Geldart and Molerus models

ρ_s = density of solid phase $(\mathrm{kg/m^3})$
ρ_a = air density $(\mathrm{kg/m^3})$
ρ_{blp} = loose-poured bulk density $(\mathrm{kg/m^3})$

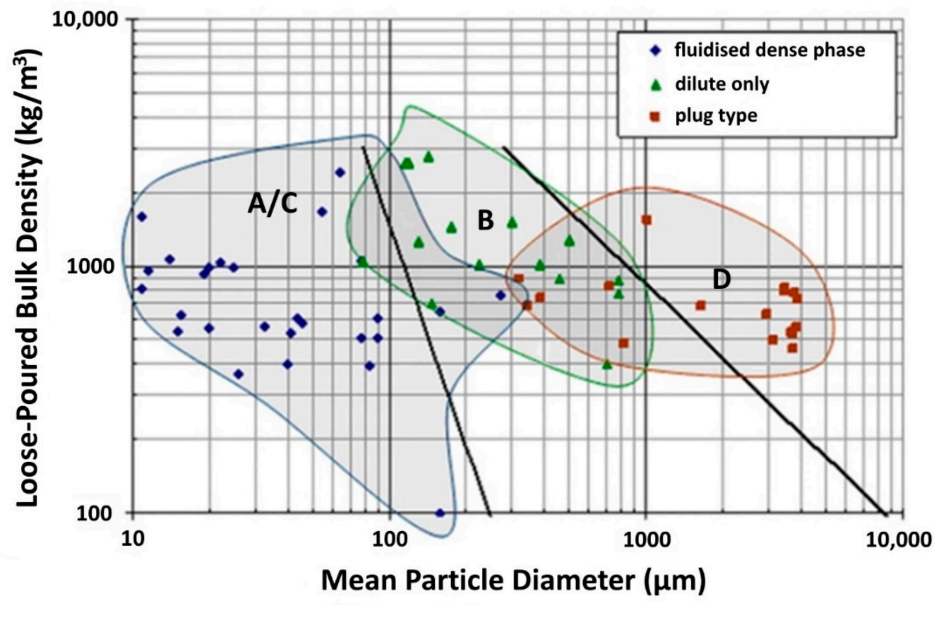

Figure 14. Modified Molerus fluidization diagram [30].

Using this diagram, the mean particle diameters and their bulk densities can help to predict their mode of flow and direct the control strategy to ensure proper transportation of the particles without exceeding the requirements.

To further characterize the particles, i.e., the influence of their shape and size, other parameters such as the sphericity (or shape factor) and the void fraction of the flow must be examined. The void fraction is the ratio between the voids present between the particles and the control volume. Reina et al. [47] determined a methodology to link these two parameters with the minimum fluidization velocities, by conducting experiments on five different types of wood particles.

The pickup velocity, which is the minimal velocity needed to set the particles in movement, is one of the most important parameters for efficient pneumatic conveying. It can be assimilated to the static friction factor in dynamics. The saltation velocity is the minimal velocity needed to keep the particles in movement [29]. It can be assimilated o the dynamic friction factor.

Fluidization velocities are the key parameter for optimal transport and are confirmed by many references [31,47,48]. The minimum fluidization velocity is characterized as the condition in which the weight of the entire bed of particles starts to be fully supported by the fluidizing gas, and with this gas velocity, the pressure drop across the bed becomes constant [48]. By forcing a flow of fluid through a quantity of solid particles, an attempt is made to carry the particles, hence transforming their state by suspending them in the fluid, either it be gas or liquid. In doing so, the mixture of solid and gas becomes a fluidlike matter and behaves according to corresponding laws of dynamics.

In order to establish the governing laws of this type of flow, a further look at recommended velocities should be explored. According to Mills [49], the recommended velocities for pneumatic conveying of coarse granular materials should be between 13 and 16 m/s. Thus, the shapes and sizes of wood particles present a high permeability and so the air velocity should be more of the order of 20 m/s (4000 feet/min), as confirmed by Bhatia [50]. This velocity translates to a Mach number of 0.06. According to White [51], this Mach number being well inferior to 0.3, the flows can be assumed to be incompressible. The behavior of the system is then assumed to be similar to hydrodynamics.

Prediction of minimum velocities of fluidized beds have been studied by many authors [9,10,26], referring back to Sabri Ergun [52] and his development of the equation that puts in relation the differential pressure, the velocity, the shape of the particles and the void fraction of the flow. The Ergun equation (Equation (6)) has been recognized to help develop accurate models of multiphase flows by dimensioning the viscous and kinetic energy losses.

This equation shows the differential pressure Δp (Pa) as a function of the bed void fraction ε_b, the gas viscosity μ_g (Ns/m^2), the gas velocity u_g (m/s), the solid particle sphericity $\varnothing_s$ and the particle average diameter d_p (m). The term L_0 refers to the height of the bed of solid particles, in the case of a vertical flow. In the case of a horizontal flow, it would correspond to a fixed length, such as 1 m, for example, [47].

$$\frac{\Delta p}{L_0} = \overbrace{\frac{150(1-\varepsilon_b)^2}{\varepsilon_b^3}\frac{\mu_g u_g}{(\varnothing_s d_p)^2}}^{\text{viscous energy loss}} + \overbrace{\frac{1.75(1-\varepsilon_b)}{\varepsilon_b^3}\frac{\rho_g u_g^2}{\varnothing_s d_p}}^{\text{kinetic energy loss}} \tag{6}$$

In considering the Ergun equation in its dimensionless form (Equation (7)), two parameters clearly stand out: the Reynold's number, and the Archimedes number. It also brings out the relation between the minimal fluidization void fraction (ε_{mf}), the solid phase density (ρ_s), the gas phase density (ρ_g), the flow velocity (u), the particle mean diameter (d) and sphericity ($\varnothing_s$), and the flow viscosity (μ). This form of the Ergun equation presents the relations between all the pertinent parameters of the multiphase flow. Ergun's equation can, thus, be rewritten as,

$$\frac{Ar}{Re} = 150\frac{1-\varepsilon_{mf}}{\varnothing_s^2\varepsilon_{mf}^3} + \frac{1.75}{\varnothing_s\varepsilon_{mf}^3}Re = \frac{d^2 g\left(\rho_s - \rho_g\right)}{u\mu} \tag{7}$$

After having identified the particles to transport and the type of flow that is best suited for this material, the physical parameters of the flow itself must be examined. The velocities and pressure differentials are of predominant importance to determine the flow conditions. To maintain a flow type, the velocities must be adjusted in order to respond to the pressure differential variations. The void fraction, the particle sphericity and size, as well as the solid and gas densities will have effects on the differential pressures of the flow. The Ergun equation can serve to evaluate the velocity adjustment necessary to maintain the fluidization of the flow.

To transport the dust from the source applications to the cyclone collector, the velocities are of primary importance and are directly controlled by the rotation speed of the motor. To adjust this rotation speed according to the dust load to extract, the differential pressures must be measured and monitored at strategic locations in the circuit. So, this being the primary parameter to consider for the evaluations of the desired adjustments, the theories of pneumatic conveying become the guiding principles of this system's analysis.

2.4. Multiphase Viscous Flow in Ducts

A dust collecting system is composed of various ducting elements that direct the collected particles to the cyclone. The typical elements are the ducts themselves, with their respective shape, size and inner surface roughness. The rest of the elements are accessories that help to link together the network, such as elbows, junctions and transition pieces. Figure 15 shows a rendering of a typical dust collecting network.

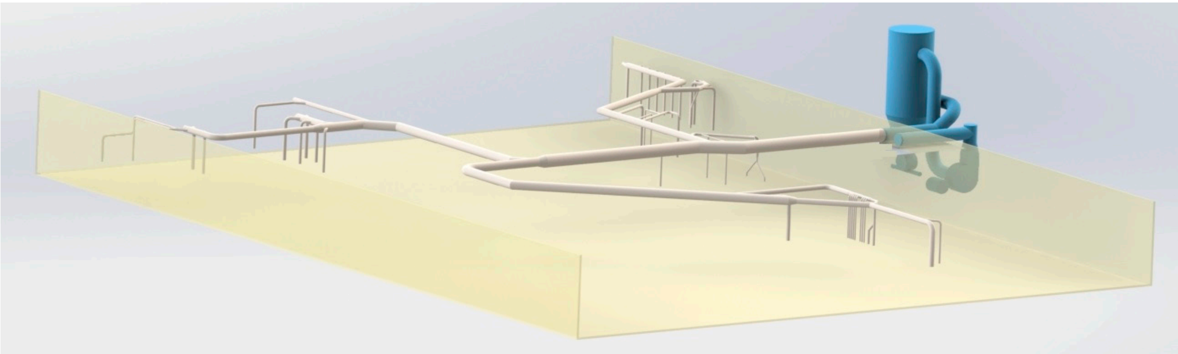

Figure 15. Dust collecting network.

The performance of the ducting network is characterized by its effects on the flow, hence the loss of transport power along the ducts. This loss is a function of the pressure drop in the ducting. This subject has been covered by many authors [48,52]. Tripathi et al. [53] rendered a study by separating the total pressure drops into components. In a multiphase flow, the two components can be added linearly as per Equation (8), where Δp_f is due to the fluid and Δp_p is due to the presence of particles.

$$\Delta p = \Delta p_f + \Delta p_p \tag{8}$$

The pressure drop due to the fluid can be calculated from Equation (9), where f_D is the Darcy friction factor of the interior surface of the pipe,

$$\Delta p_f = f_D \frac{\rho_f}{2} \frac{u_f^2}{D} L \tag{9}$$

where

Δp is in Pa
ρ_f is in kg/m^3
u_f is in m/s
L and D are in m.

Many studies [48,52,54–58] were conducted to determine more precisely the friction factor according to the surface roughness of the piping used. According to many fluid mechanics manuals such as White [51], the most widely used study is from Moody [59], which gave us the Moody chart for evaluating the friction factor of a single-phase flow in a pipe. In the case of multiphase flow, this chart has not proven to be applicable. This remains to be researched and an adjusted chart could represent an interesting objective for a study project.

To determine the pressure drop in the solid phase of the flow, as mentioned in Section 2.3, the flow must be characterized according to its density, thereby determining if it is dilute or dense.

If it is dilute, the Langrangian method will be used and the particles will be analyzed as per their force and velocity profiles [60]. The particle is assumed to be spherical and is considered as a point mass, with forces acting on it. Figure 16 shows a sketch of a typical particle with all the forces acting on it, where F_g is the force of gravity, F_A is the Archimedes force, defined as the upward buoyant force exerted on a particle immersed in a fluid and is equal to the weight of the fluid occupied by the particle [51], F_L is the lift force, F_D is the drag force and v_r is the resultant velocity of the particle.

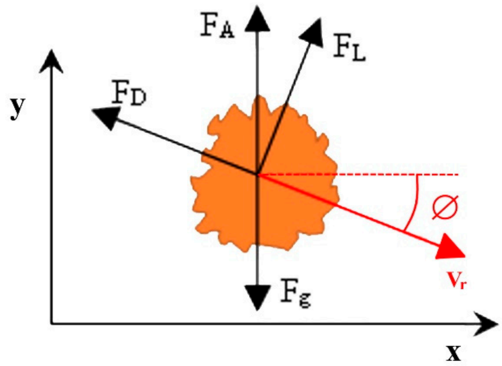

Figure 16. Force diagram of a particle.

The equations of motion will be derived from an analysis of equilibrium of a point mass. By considering the effects along the horizontal axis, we can observe that the resultant force is a result of the drag and lift forces acting on the particle.

$$\sum F_x = ma_x \tag{10}$$

$$F_L \sin \varnothing - F_D \cos \varnothing = ma_x \tag{11}$$

The same analysis in the vertical axis shows the combined effect of the three forces, F_L, F_g and F_A on the motion of the particle.

$$\sum F_y = ma_y \tag{12}$$

$$F_A + F_L \cos \varnothing + F_D \sin \varnothing - F_g = ma_y \tag{13}$$

From the definitions of these four forces, we can see influential parameters appear.

$$F_g = \rho_p V_p g \tag{14}$$

where suffix p stands for particle, and V_p is further defined as the spherical particle volume

$$V_p = \frac{1}{6}\pi d_p^3 \tag{15}$$

The lift and drag forces are defined as

$$F_L = \frac{1}{2}\rho_a A_p C_L v_p^2 \tag{16}$$

$$\text{and } F_D = \frac{1}{2}\rho_a A_p C_D v_p^2 \tag{17}$$

$$\text{where } C_D = \frac{Re_D}{24} = \frac{v_p d_p}{24\nu_a} \tag{18}$$

where

F_L and F_D are respectively the lift and drag forces in N
ρ_a is the air density in kg/m^3
A_p is the mean cross-section of the particle in m^2
C_L and C_D are the lift and drag coefficients, and
v_p is the particle velocity in m/s.

The lift force on a particle in a multiphase flow is negligible compared to the drag and gravity forces, if we consider that the particles in the axial flow of air will adopt a position that will give them an approximate symmetry with respect to a vertical and a horizontal plane. In such a case, we can assume that the particles are subjected to drag forces only [51], and thus the lift coefficient is omitted [61]. As pointed out by Schellander [34], if the multiphase flow is considered to be dense, the Eulerian method of modeling is recommended.

Any dust collecting system is basically composed of a typical matrix element of two pipes joining into one. Figure 17 shows this element of which the whole network can be drawn as a combination of many such elements. From this we can deduce that the principles of conservation of mass can be applied as per Equation (8), and according to the Reynolds transport theorem.

$$\rho A_1 v_1 = \rho A_2 v_2 + \rho A_3 v_3 \tag{19}$$

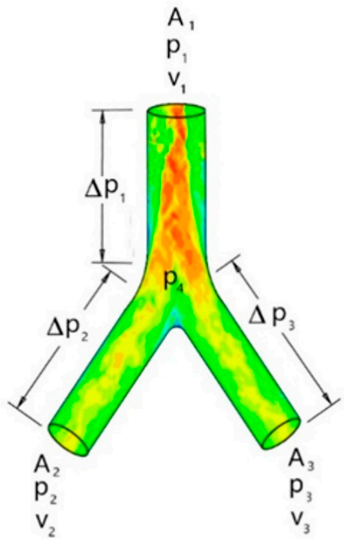

Figure 17. Typical mesh element.

In a dust collecting system the entry volumes are at points 2 and 3, and the outlet volume is at point 1. This typical control volume can be used as the basis for the elaboration of the matrices that will be used to develop the model of the system. The model will render velocity profiles to maintain at each dust collection inlet, to assure proper transport, so as to guarantee a dust free work environment for the surrounding workers. The velocity being a function of the pressure differential, the following expressions describe this relation:

$$\begin{aligned} \rho A_1 v_1 &= c_1(p_4 - p_1) \\ \rho A_2 v_2 &= c_2(p_2 - p_4) \\ \rho A_3 v_3 &= c_3(p_3 - p_4) \end{aligned} \tag{20}$$

Since the density and the conduit areas are known and static, we can transfer these two parameters into the constants c_i and (18) becomes

$$c_i' \Delta p_i = v_i \tag{21}$$

and a matrix system can be derived

$$\begin{bmatrix} c'_1 \\ c'_2 \\ c'_3 \\ \vdots \\ c'_i \end{bmatrix} \begin{bmatrix} \Delta p_1 \\ \Delta p_2 \\ \Delta p_3 \\ \vdots \\ \Delta p_i \end{bmatrix} = \begin{bmatrix} v_1 \\ v_2 \\ v_3 \\ \vdots \\ v_i \end{bmatrix} \tag{22}$$

We want to guaranty a sufficient transport velocity at each pickup inlet, so the matrices system will verify that

$$\forall v_i \; \geq v_{min} \pm \text{margin} \tag{23}$$

2.5. Synopsis

In this review and in Beaulac et al. [62], influencing parameters have been studied. [62] presents energy efficiency optimizations when designing or physically modifying dust collection systems. One of the recommendations points out variable frequency drives coupled with high-efficiency motors, which implies considerable investments but can prove to be a cost-saving optimization well worth looking into. The previous recommendation, coupled with improved maintenance routines seem to be the most important improvements that can be brought to a dust collection system.

In the present article, the operating parameters are outlined and studied in order to find the most influencing ones. Section 2.2 points out the influencing parameters that pertain to the cyclone: the inlet velocity and the pressure drop between the inlet and the outlet are the two most important parameters. Section 2.3 outlines the influencing parameters for the pneumatic transport of the particles, from their origin points to the cyclone. Again, the velocities and pressure drops are of considerable importance, but another parameter presents an influence, the density of the material being transported. All three parameters influence each other and need to be considered as such.

Section 2.4 looks at multiphase flows in a ducting network of the complexities present in a dust collection system. A matrix can be deduced, and we can thereby conclude that the velocities must be controlled in order to maintain a sufficient transport performance. Ultimately, we can evaluate the velocity v_i at each moment—this velocity being the actual air-dust mixture velocity at the dust collector entry and, hence, in direct relation to the driving motor's speed, which is what we can control in such a system.

3. Conclusions

Dense phase pneumatic conveying may be defined as the fluidization of solid particles in a gas flow along a network of pipe filled with solids at one or more cross-sections [10,27]. Two types of dense phase transport conditions have been identified, the fluidized dense phase and the plug-type dense phase. Many industrial applications use the concept of pneumatic conveying, such as dust collecting systems, for example.

It is widely assumed in the literature review that the optimal configuration of the pneumatic conveying will depend on the flow pattern of the particles in the pipes. Dense phase transport is pointed out as being more efficient [30].

The next step in optimizing dust collecting systems is to determine the shape and size of the particles to transport. Geldart [40], Molerus [42] and Pan [43] contributed largely to this effect. Jones and Williams established a comparison table [30] in order to better appreciate the influence of these parameters.

From the flow pattern and particle parameters, the calculation methods can be assessed to determine the best suited method for the problem at hand. Hence, the primary influential parameters driving the dust collection systems are the velocities of the multiphase flow, and the pressure differentials [29,30,47,48], which are dependent of the velocities. They depend on the properties of the transporting fluid and of the transported particles. The determination of the relationship between these two fundamental parameters further drives the model that can serve to develop a control strategy that can efficiently adjust the system's power consumption, and hence permit operation costs savings and environmental benefits, depending on the energy production method of the systems operation region.

Further developments in control strategies that take into account the parameters outlined by this literature review would lead to the accomplishment of the main goal presented, i.e., the energy efficiency of industrial systems. From reference [4] by Bunse, much research work needs to be developed in regards to energy efficiency and it's monitoring. One can refer to the article to acknowledge all the aspects of research that are yet to be explored, and a future article from the authors of this paper will be presented, outlining some of the recommendations of Bunse.

Author Contributions: Conceptualization, P.B.; methodology, P.B., M.I., A.I. and J.B.; validation, A.I. and J.B.; formal analysis, A.I. and J.B.; writing—original draft preparation, P.B.; writing—review and editing, M.I., A.I. and J.B.; visualization, M.I., A.I. and J.B.; supervision, A.I. and J.B.; project administration, A.I. and J.B.; funding acquisition, A.I. and J.B. All authors have read and agreed to the published version of the manuscript.

Funding: This research received no external funding.

Data Availability Statement: Not applicable.

Conflicts of Interest: The authors declare no conflict of interest. The funders had no role in the design of the study; in the collection, analyses, or interpretation of data; in the writing of the manuscript, or in the decision to publish the results.

References

1. Total Energy. Available online: https://www.eia.gov/totalenergy/data/browser (accessed on 30 December 2021).
2. Conti, J.; Holtberg, P.; Diefenderfer, J.; LaRose, A.; Turnure, J.T.; Westfall, L. *International Energy Outlook 2016 with Projections to 2040*; USDOE Energy Information Administration (EIA): Washington, DC, USA, 2016.
3. Energy. Our World in Data. 2015. Available online: https://ourworldindata.org/energy (accessed on 24 April 2019).
4. Bunse, K.; Vodicka, M.; Schönsleben, P.; Brülhart, M.; Ernst, F.O. Integrating energy efficiency performance in production management–gap analysis between industrial needs and scientific literature. *J. Clean. Prod.* **2011**, *19*, 667–679. [CrossRef]
5. Kaya, D.; Phelan, P.; Chau, D.; Sarac, H.I. Energy conservation in compressed-air systems. *Int. J. Energy Res.* **2002**, *26*, 837–849. [CrossRef]
6. Close, C.M.; Frederick, D.K.; Newell, J.C. *Modeling and Analysis of Dynamic Systems*; John Wiley & Sons Inc.: New York, NY, USA, 2002; p. 576.
7. Naidu, D.S.; Rieger, C.G. Advanced control strategies for heating, ventilation, air-conditioning, and refrigeration systems—An overview: Part I: Hard control. *HVAC&R Res.* **2011**, *17*, 2–21.
8. Naidu, D.S.; Rieger, C.G. Advanced control strategies for HVAC&R systems—An overview: Part II: Soft and fusion control. *HVAC&R Res.* **2011**, *17*, 144–158.
9. Clarke, K.L.; Pugsley, T.; Hill, G.A. Fluidization of moist sawdust in binary particle systems in a gas–solid fluidized bed. *Chem. Eng. Sci.* **2005**, *60*, 6909–6918. [CrossRef]
10. Kunii, D.; Levenspiel, O. *Fluidization Engineering*, 2nd ed.; Butterworth-Heinemann: Stoneham, MA, USA, 1991.
11. Klinzing, G.E. Historical Review of Pneumatic Conveying. *KONA Powder Part. J.* **2018**, *35*, 150–159. [CrossRef]
12. Twin Lobe High Pressure Blowers. Available online: https://www.indiamart.com/proddetail/twin-lobe-high-pressure-blowers-10456367788.html (accessed on 30 April 2019).
13. Leith, D.; Mehta, D. Cyclone performance and design. *Atmos. Environ.* **1973**, *7*, 527–549. [CrossRef]
14. Azadi, M.; Azadi, M. An analytical study of the effect of inlet velocity on the cyclone performance using mathematical models. *Powder Technol.* **2012**, *217*, 121–127. [CrossRef]
15. Shepherd, C.B.; Lapple, C.E. Flow Pattern and Pressure Drop in Cyclone Dust Collectors. *Ind. Eng. Chem.* **1939**, *31*, 972–984. [CrossRef]
16. Ter Linden, A.J. Investigations into Cyclone Dust Collectors. *Proc. Inst. Mech. Eng.* **1949**, *160*, 233–251. [CrossRef]
17. Ferguson, R.I.; Church, M. A Simple Universal Equation for Grain Settling Velocity. *J. Sediment. Res.* **2004**, *74*, 933–937. [CrossRef]
18. Dirgo, J.; Leith, D. Cyclone Collection Efficiency: Comparison of Experimental Results with Theoretical Predictions. *Aerosol Sci. Technol.* **2007**, *4*, 401–415. [CrossRef]
19. Azadi, M.; Azadi, M.; Mohebbi, A. A CFD study of the effect of cyclone size on its performance parameters. *J. Hazard. Mater.* **2010**, *182*, 835–841. [CrossRef] [PubMed]
20. Wang, B.; Xu, D.L.; Chu, K.W.; Yu, A.B. Numerical study of gas–solid flow in a cyclone separator. *Appl. Math. Model.* **2006**, *30*, 1326–1342. [CrossRef]

21. Huang, A.-N.; Ito, K.; Fukasawa, T.; Fukui, K.; Kuo, H.-P. Effects of particle mass loading on the hydrodynamics and separation efficiency of a cyclone separator. *J. Taiwan Inst. Chem. Eng.* **2018**, *90*, 61–67. [CrossRef]
22. Coker, A.K. Understand cyclone design. *Chem. Eng. Prog.* **1993**, *89*, 51–55.
23. Funk, P.A.; Elsayed, K.; Yeater, K.M.; Holt, G.A.; Whitelock, D.P. Could cyclone performance improve with reduced inlet velocity? *Powder Technol.* **2015**, *280*, 211–218. [CrossRef]
24. Gimbun, J.; Chuah, T.G.; Fakhru'l-Razi, A.; Choong, T.S.Y. The influence of temperature and inlet velocity on cyclone pressure drop: A CFD study. *Chem. Eng. Process. Process Intensif.* **2005**, *44*, 7–12. [CrossRef]
25. Shepherd, C.; Lapple, C. *Air Pollution Control: A Design Approach*, 2nd ed.; Woveland Press Inc.: Long Grove, IL, USA, 1939; pp. 127–139.
26. Klinzing, G.E. A review of pneumatic conveying status, advances and projections. *Powder Technol.* **2018**, *333*, 78–90. [CrossRef]
27. Subramanian, R.S. Flow through Packed and Fluidized Beds. In *Department of Chemical and Biomolecular Engineering*; Clarkson University: Potsdam, NY, USA, 2002.
28. Gidaspow, D. *Multiphase Flow and Fluidization*; Academic Press Inc.: San Diego, CA, USA, 1994; p. 467.
29. Gomes, L.M.; Mesquita, A.L. On the prediction of pickup and saltation velocities in pneumatic conveying. *Braz. J. Chem. Eng.* **2014**, *31*, 35–46. [CrossRef]
30. Jones, M.G.; Williams, K.C. Predicting the mode of flow in pneumatic conveying systems—A review. *Particuology* **2008**, *6*, 289–300. [CrossRef]
31. Thomson, W.J. *Transport Phenomena*; Prentice Hall: Upper Saddle River, NJ, USA, 2000; p. 509.
32. Abdullah, E.C.; Geldart, D. The use of bulk density measurements as flowability indicators. *Powder Technol.* **1999**, *102*, 151–165. [CrossRef]
33. Obie, O. Density Measurement of Multiphase Pipe Flows. Ph.D. Thesis, University of Huddersfield, Huddersfield, UK, 2017; p. 350.
34. Schellander, D. *CFD Simulations of Particle Laden Flows*; Anchor Academic Plublishing: Hamburg, Germany, 2013; p. 143.
35. Manjula, E.V.P.J.; Hiromi Ariyaratne, W.K.; Ratnayake, C.; Melaaen, M.C. A review of CFD modelling studies on pneumatic conveying and challenges in modelling offshore drill cuttings transport. *Powder Technol.* **2017**, *305*, 782–793. [CrossRef]
36. Lun, C.K.K.; Savage, S.B.; Jeffrey, D.J.; Chepurniy, N. Kinetic theories for granular flow inelastic particles in Couette flow and slightly inelastic particles in a general flowfield. *J. Fluid Mech.* **1984**, *140*, 223–256. [CrossRef]
37. Wen, C.-Y.; Simons, H.P. Flow characteristics in horizontal fluidized solids transport. *AIChE J.* **1959**, *5*, 263–267. [CrossRef]
38. Dhodapkar, S.V.; Klinzing, G.E. Pressure fluctuations in pneumatic conveying systems. *Powder Technol.* **1993**, *74*, 179–195. [CrossRef]
39. Williams, K.C. *Dense Phase Pneumatic Conveying of Powders: Design Aspects and Phenomena chap1-2, in School of Engineering*; University of Newcastle: Newcastle, Australia, 2008; p. 60.
40. Geldart, D. Types of gas fluidization. *Powder Technol.* **1972**, *7*, 285–292. [CrossRef]
41. Dixon, G. The impact of powder properties on dense phase flow. In Proceedings of the International Conference on Penumatic Conveying, London, UK, 16–18 January 1979.
42. Molerus, O. Interpretation of Geldart's Type A, B, C and D Powders by Taking Into Account Interparticle Cohesion Froces. *Powder Technol.* **1982**, *33*, 81–87. [CrossRef]
43. Pan, R. Material properties and flow modes in pneumatic conveying. *Powder Technol.* **1999**, *104*, 157–163. [CrossRef]
44. Bulk Density. Available online: https://en.wikipedia.org/wiki/Bulk_density (accessed on 11 November 2021).
45. Godard, K.; Richardson, J.F. Bubble velocities and bed expansions in freely bubbling fluidised beds. *Chem. Eng. Sci.* **1969**, *24*, 663–670. [CrossRef]
46. Williams, K.; Jones, M. Classification diagrams for dense phase pneumatic conveying. *Powder Handl. Process.* **2003**, *15*, 368–373.
47. Reina, J.; Velo, E.; Puigjaner, L. Predicting the minimum fluidization velocity of polydisperse mixtures of scrap-wood particles. *Powder Technol.* **2000**, *111*, 245–251. [CrossRef]
48. Xu, C.C.; Zhu, J. Prediction of the Minimum Fluidization Velocity for Fine Particles of Various Degrees of Cohesiveness. *Chem. Eng. Commun.* **2008**, *196*, 499–517. [CrossRef]
49. Mills, D. *Pneumatic Conveying Design Guide*, 2nd ed.; Elsevier Butterworth-Heinemann: Burlington, MA, USA, 2004; p. 637.
50. Bhatia, A. Pneumatic Conveying Systems. In *Chemical Engineering*; Continuing Education and Development, Inc.: Stony Point, NY, USA, 2019; pp. 1–57.
51. White, F.M. *Fluid Mechanics*, 8th ed.; McGraw-Hill: New York, NY, USA, 2016; p. 848.
52. Ergun, S. Fluid Flow Through Packed Columns. *Chem. Eng. Prog.* **1952**, *48*, 89–94.
53. Tripathi, N.M.; Levy, A.; Kalman, H. Acceleration pressure drop analysis in horizontal dilute phase pneumatic conveying system. *Powder Technol.* **2018**, *327*, 43–56. [CrossRef]
54. Colebrook, C.F.; Blench, T.; Chatley, H.; Essex, E.H.; Finniecome, J.R.; Lacey, G.; Williamson, J.; Macdonald, G.G. Correspondence. Turbulent flow in pipes, with particular reference to the transition region between the smooth and rough pipe laws. (Includes plates). *J. Inst. Civ. Eng.* **1939**, *12*, 393–422. [CrossRef]
55. Kamand, F.Z. Hydraulic Friction Factors for Pipe Flow. *J. Irrig. Drain. Eng.* **1988**, *114*, 311–323. [CrossRef]
56. McKeon, B.J.; Swanson, C.J.; Zagarola, M.V.; Donnelly, R.J.; Smits, A.J. Friction factors for smooth pipe flow. *J. Fluid Mech.* **2004**, *511*, 41–44. [CrossRef]

57. Herwig, H.; Gloss, D.; Wenterodt, T. A new approach to understanding and modelling the influence of wall roughness on friction factors for pipe and channel flows. *J. Fluid Mech.* **2008**, *613*, 35–53. [CrossRef]
58. Kiijarvi, J. Darcy friction factor formulae in turbulent pipe flow. *Lunowa Fluid Mech. Pap.* **2011**, *110727*, 1–11.
59. Moody, L.F. Friction Factors for Pipe Flow. *Trans. ASME* **1944**, *66*, 671–684.
60. Martini, F.; Ramdenee, D.; Ibrahim, H.; Ilinca, A. A Lagrangean Interactive Interface to Evaluate Ice Accretion Modeling on a Cylinder—A test case for icing modeling on wind turbine airfoils. In Proceedings of the 2011 IEEE Electricl Powerr and Energy Conference, Winnipeg, MB, Canada, 3–5 October 2011; pp. 456–461.
61. Soo, S.L. Dynamics of Multiphase Flow Systems. *Ind. Eng. Chem. Fundam.* **1965**, *4*, 426–433. [CrossRef]
62. Beaulac, P.; Issa, M.; Ilinca, A.; Lepage, R.; Martini, F. Improving the Energy Efficiency of Cyclone Dust Collectors for Wood Product Factories. *Open J. Energy Effic.* **2021**, *10*, 97–119. [CrossRef]